Supplement of Atmos. Chem. Phys., 26, 2985–3000, 2026
https://doi.org/10.5194/acp-26-2985-2026-supplement

Atmospheric Chemistry and Physics
Open Access

Supplement of

Contrasting aerosol mixing states at inland and coastal sites: an entropy-based metric for CCN activity

Jingye Ren et al.

Correspondence to: Ru-Jin Huang (rujin.huang@ieecas.cn) and Fang Zhang (zhangfang2021@hit.edu.cn)

Supplementary Figures

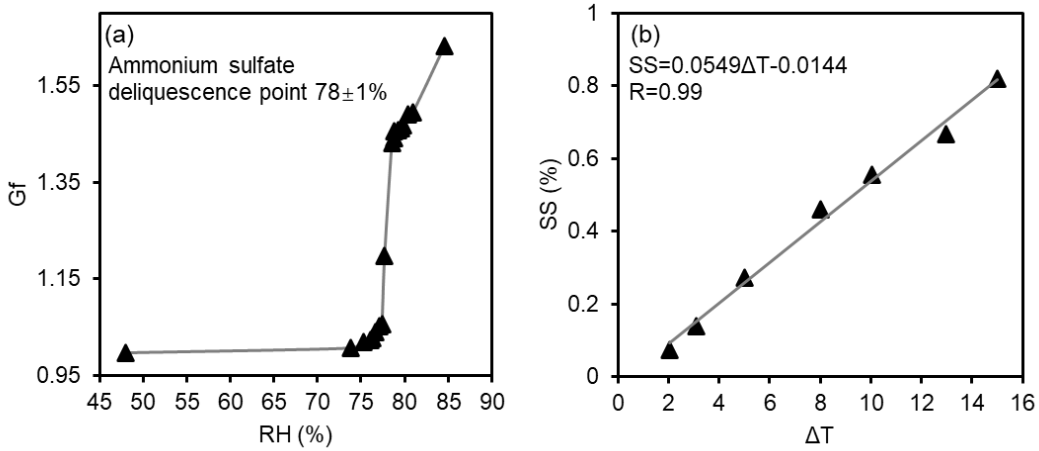

Fig S1. Example of calibration results of HTDMA and CCN used in this study, (a) Humid gram of ammonium sulfate for 150-nm particles measured with HTDMA, (b) Variation of supersaturation as function of Delta temperature for ammonium sulfate aerosol.

The HTDMA system was regularly calibrated with ammonium sulfate solution for RH calibration. Fig. S1a gives the calibration result in IAP site as an example. The deliquescence point of ammonium sulfate is 78±1 %, which is consistent with previous studies (Tan et al., 2013). The CCN-100 was calibrated with ammonium sulfate for column supersaturation as suggested by Rose et al. (2008). Fig. S1b shows the supersaturation (SS) levels of the CCNc with longitudinal temperature differences of 2, 3, 5, 8, 10, 13, and 15K. Based on this calibration, five effective SS levels were 0.12, 0.14, 0.23, 0.40, and 0.76 %. Similar calibrations were operated in the measurements during MHD site (Xu et al., 2021).

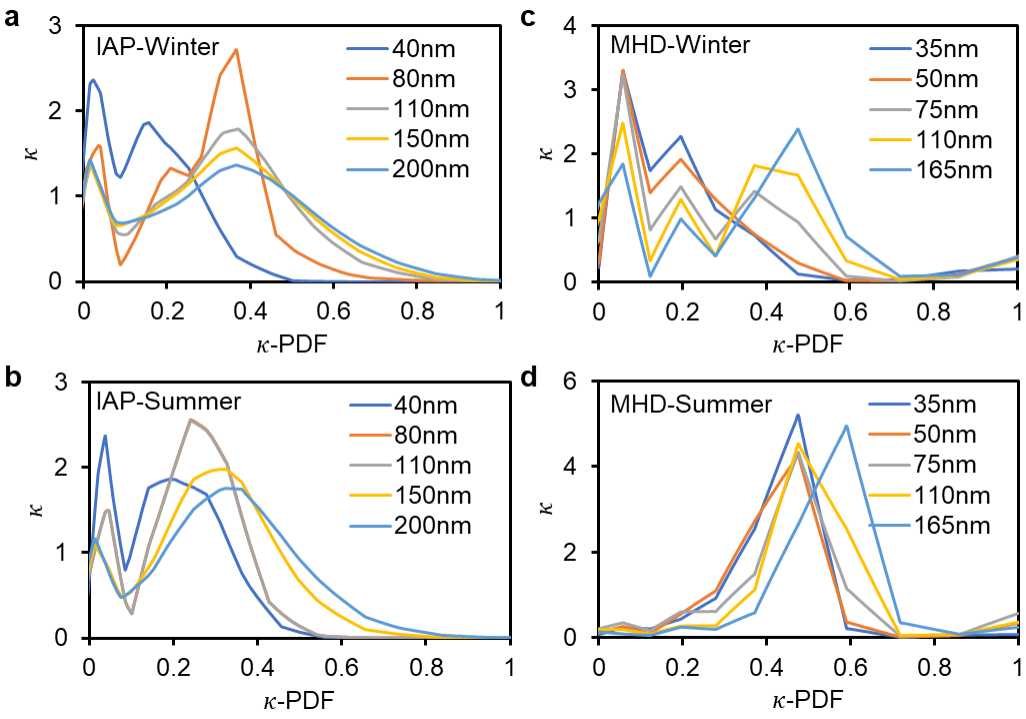

40

41 **Fig S2.** Mean value of the κ–PDF for aerosols of five diameters during winter and

42 summer periods at IAP (a and b) and MHD (c and d) sites.

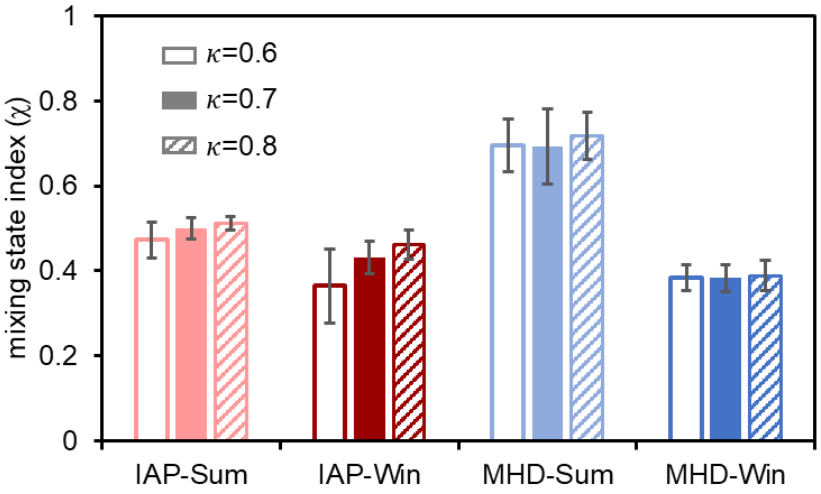

43

44 **Fig S3.** Sensitivity of the hygroscopic parameter for the group of the hygroscopic

45 species on the mixing state index χ.

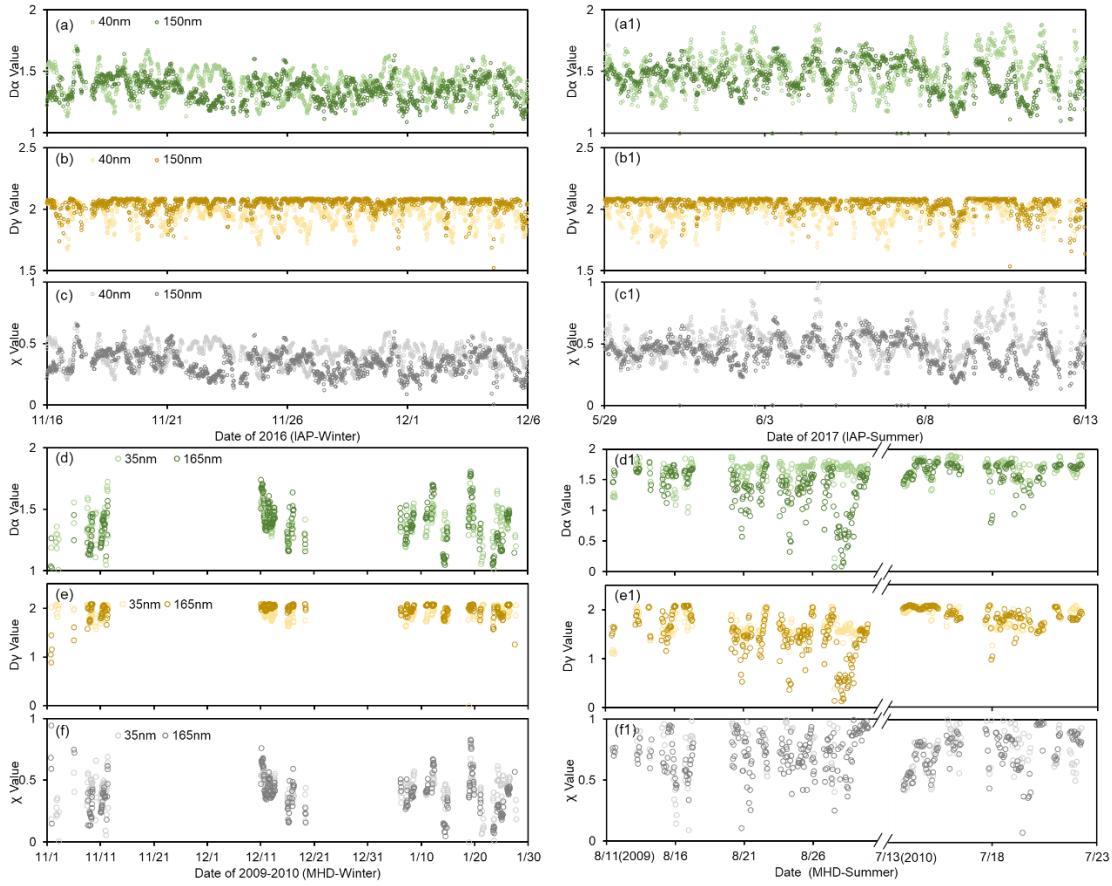

Fig S4. Time series of the average per-particle species diversity Dα, the bulk population species diversity Dγ, and their affine ratio χ. During winter and summer periods at IAP and MHD sites.

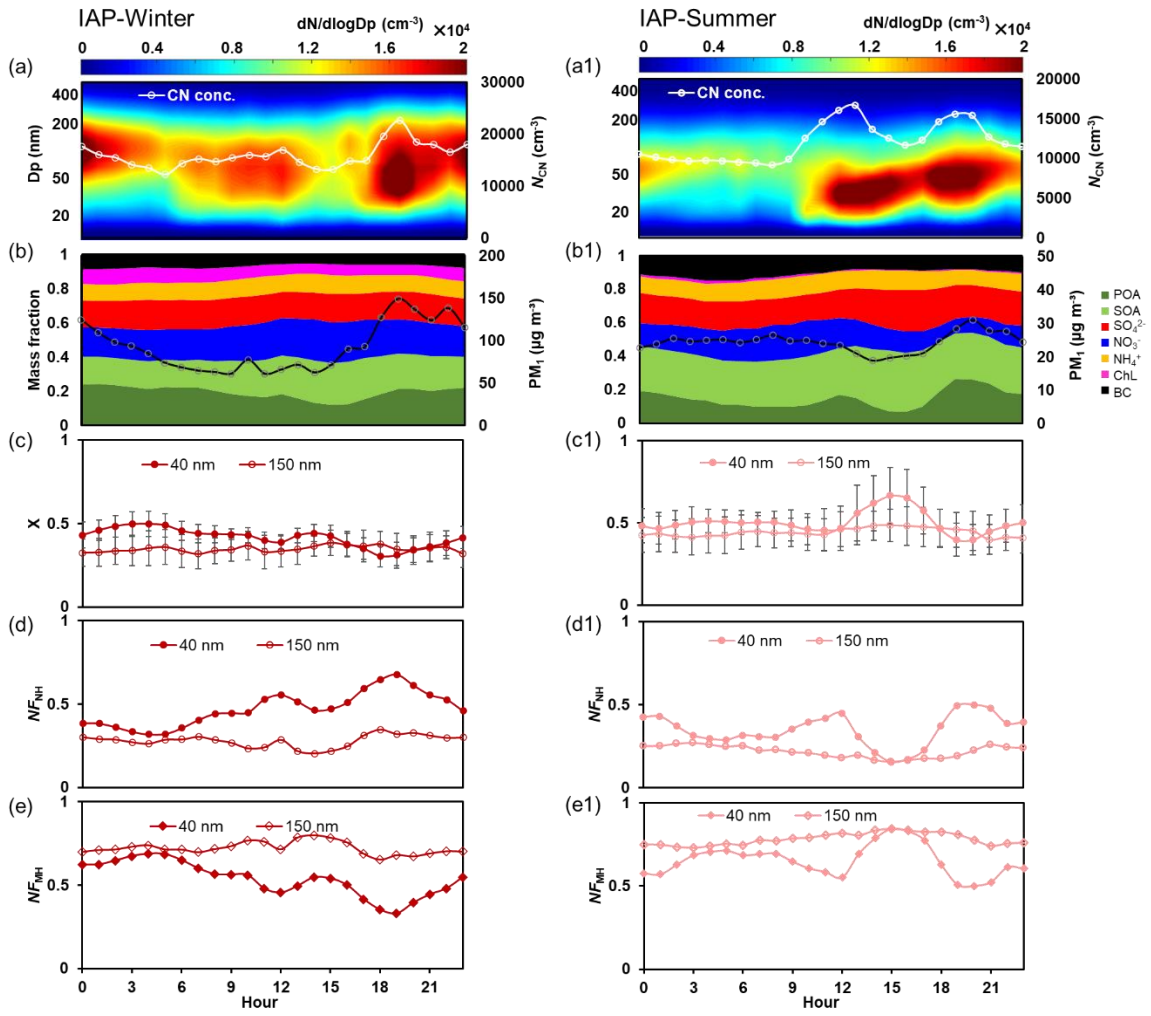

Fig S5. Diurnal variation of the particle number size distribution and CN number concentration during winter (a) and summer periods at IAP site (a1), particle matter concentration and mass fraction of the chemical components (b and b1), the mixing state index (χ) at 40 and 150 nm (c and c1), number fraction of nearly hydrophobic mode (NH) (d and d1) and more hygroscopic mode (MH) particles (e and e1).

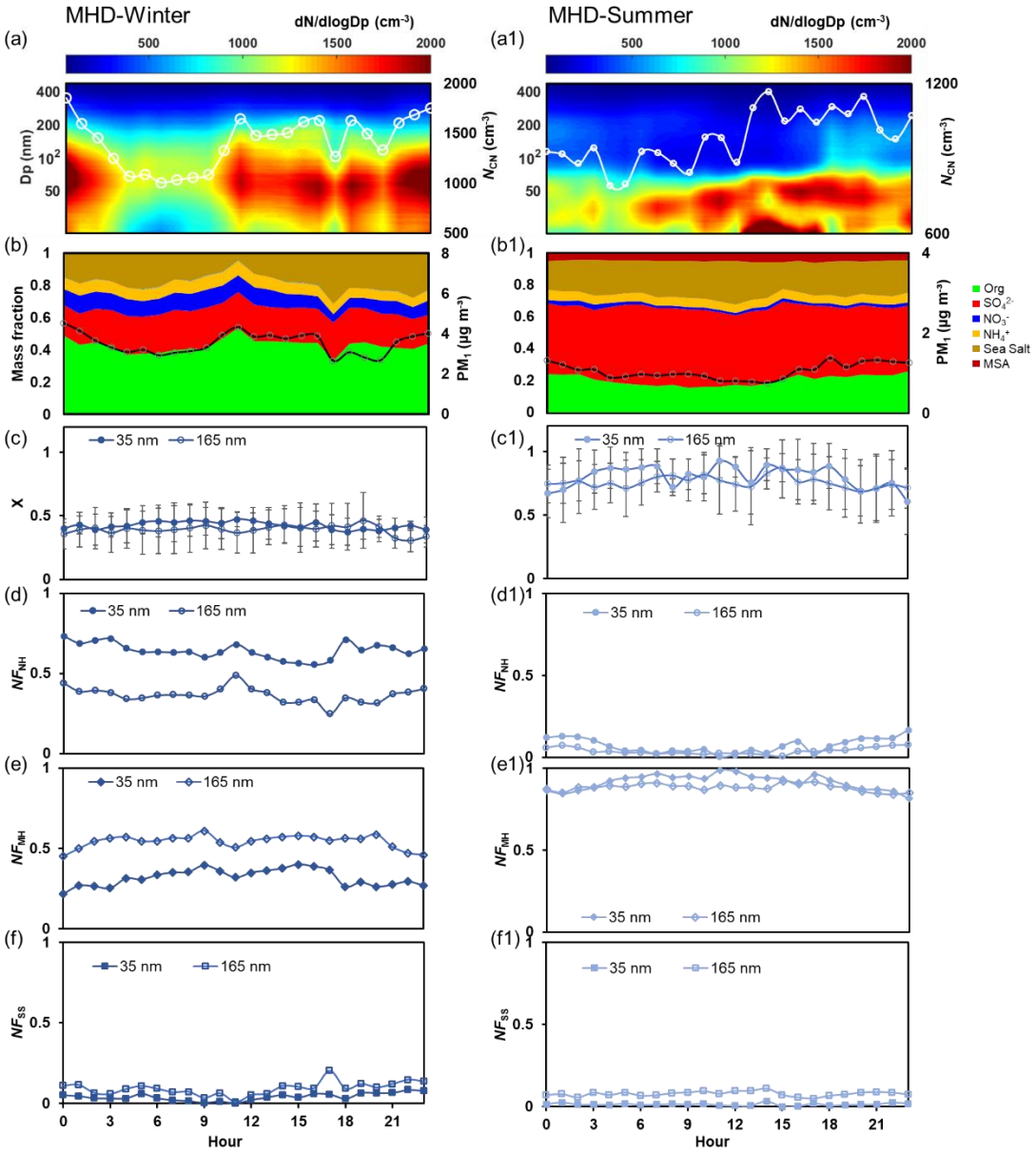

Fig S6. Diurnal variation of the particle number size distribution and CN number concentration during winter (a) and summer periods at MHD site (a1), particle matter concentration and mass fraction of the chemical components (b and b1), the mixing state index (χ) at 35 and 165 nm (c and c1), number fraction of nearly hydrophobic mode (NH) (d and d1), more hygroscopic mode (MH) (e and e1) and sea salt mode (SS) particles (f and f1).

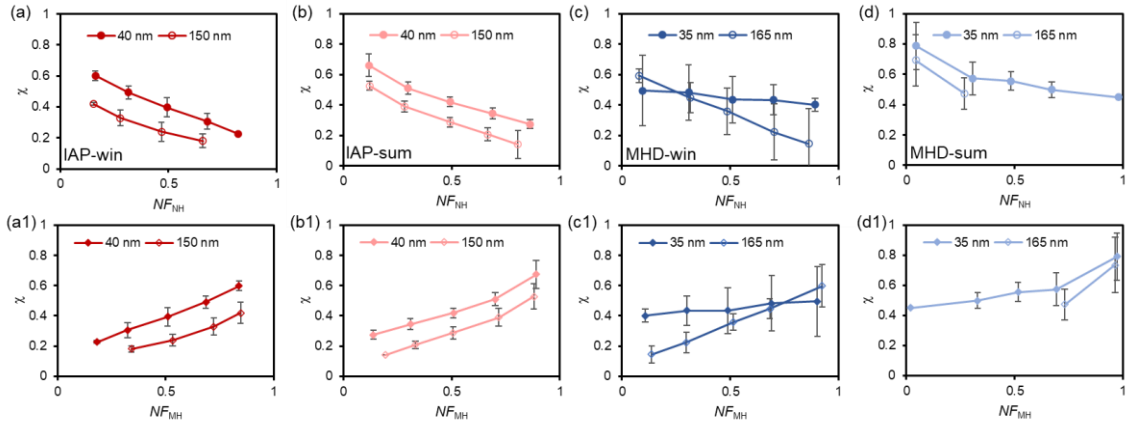

63

64 **Fig S7.** Mixing state (χ) as a function of number fraction of the nearly hydrophobic

65 mode (a) and more hygroscopic mode (a1) in IAP-winter; (b) and (b1) in IAP-summer;

66 (b) and (b1) in IAP-summer; (d) and (d1) in MHD-summer.

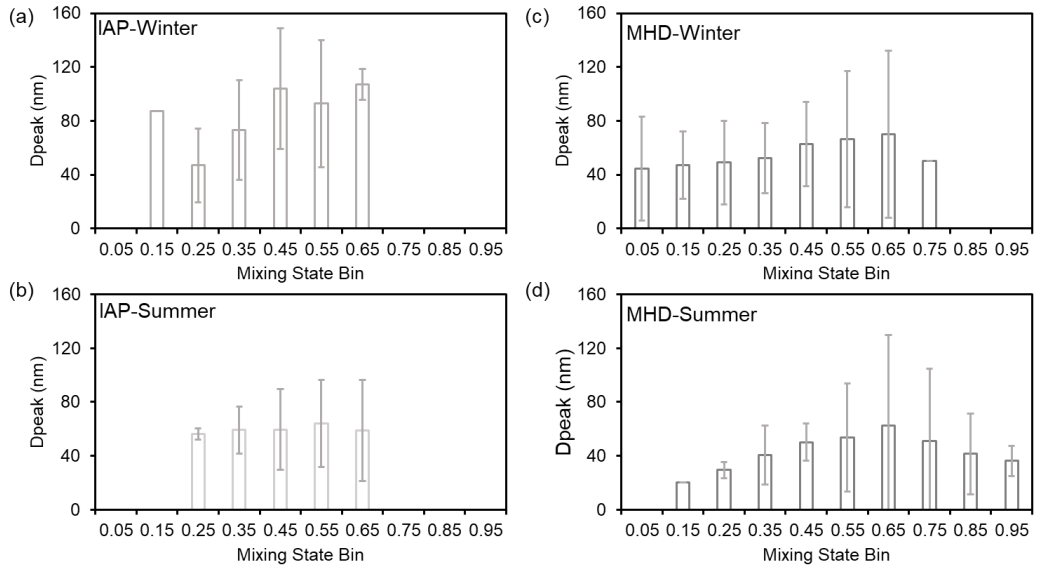

67

68 **Fig S8.** Variation of the peak diameter (D_{peak}) with the mixing state index at the step of

69 0.1 during winter and summer periods in IAP (a and b) and MHD sites (c and d).

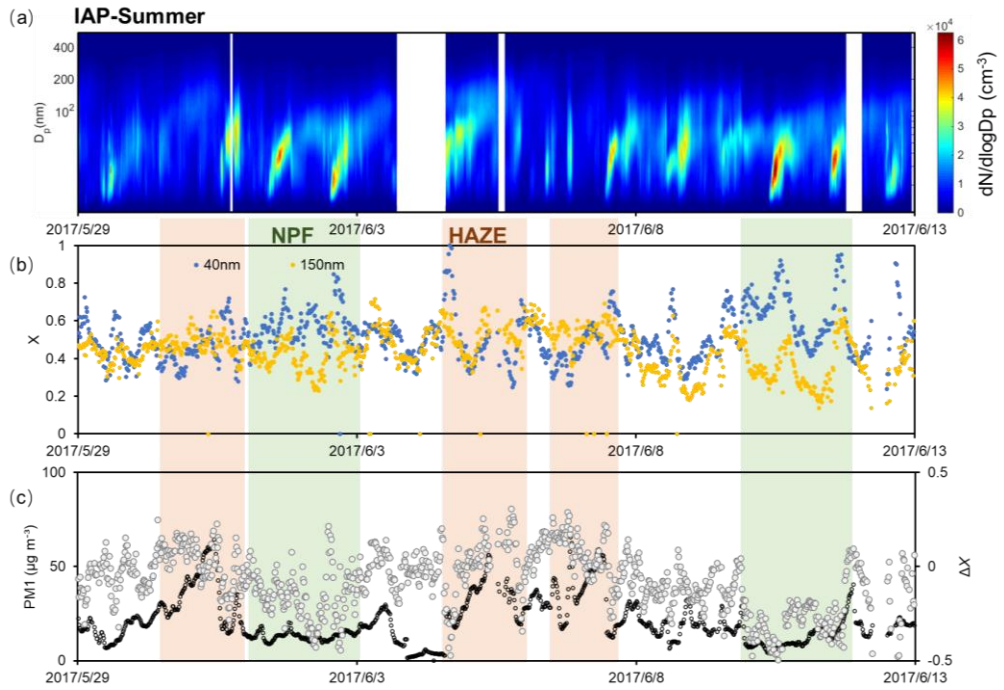

Fig S9. Time series of the particle number size distribution (a), χ for 40 and 150 nm (b), particle matter mass concentration and the difference of χ between 150 and 40 nm (c).

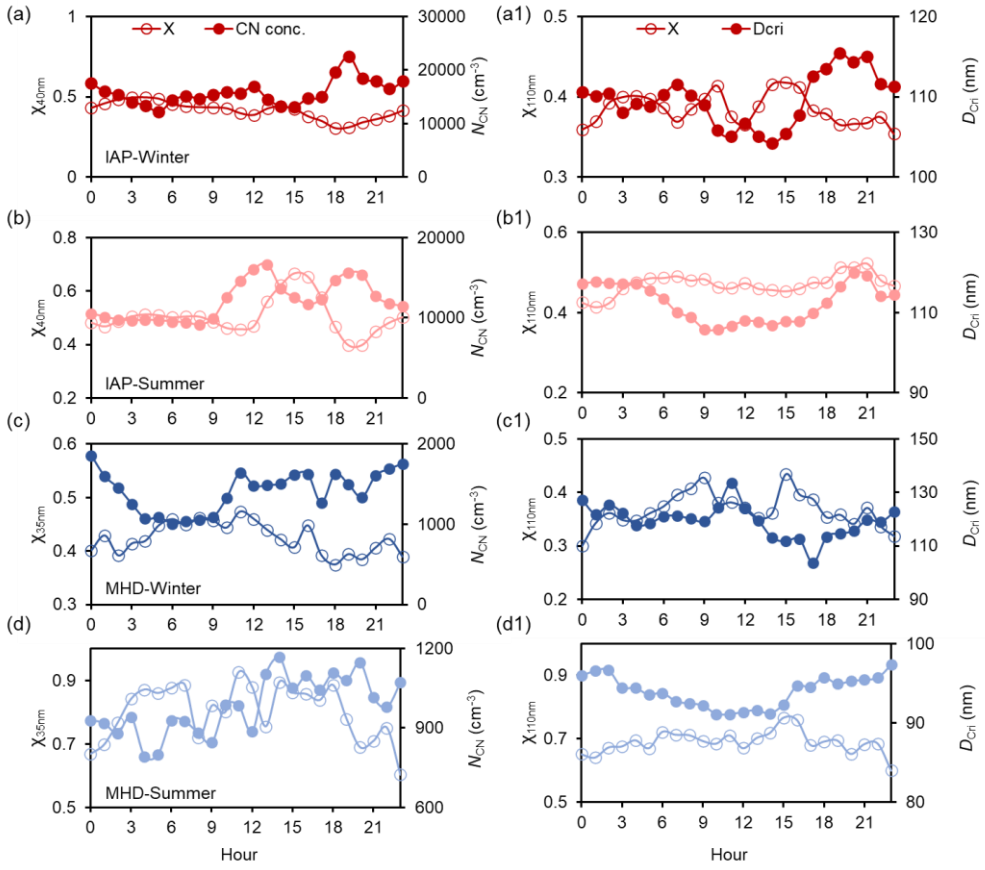

Fig S10. Diurnal variation of χ and CN concentration during winter and summer periods

for 40 nm and 150 nm aerosols at IAP and for 35 nm and 165 nm aerosols at MHD site.

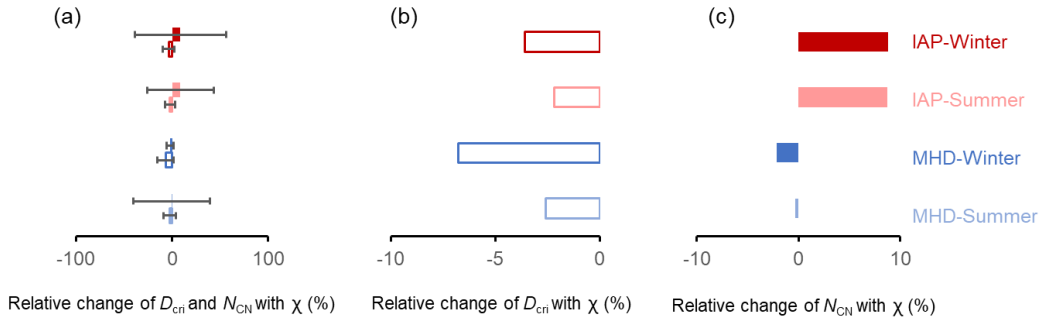

Fig S11. Relative change of the critical diameter and CN concentration with the mixing state index χ in IAP-winter, IAP-summer, MHD-winter and MHD-summer.

References

Tan, H., Xu, H., Wan, Q., Li, F., Deng, X., Chan, P. W., Xia, D., and Yin, Y.: Design and application of an unattended multifunctional H-TDMA system, J. Atmos. Ocean. Tech., 30, 1136–1148, https://doi.org/10.1175/JTECH-D-12-00129.1, 2013.

Rose, D., Gunthe, S. S., Mikhailov, E., Frank, G. P., Dusek, U., Andreae, M. O., Pöschl, U.: Calibration and measurement uncertainties of a continuous-flow cloud condensation nuclei counter (DMT-CCNC): CCN activation of ammonium sulfate and sodium chloride aerosol particles in theory and experiment, Atmospheric Chemistry and Physics., 8(5), 1153–1179, https://doi.org/10.5194/acp-8-1153-2008, 2008.

Xu, W., Ovadnevaite, J., Fossum, K. N., Lin, C., Huang, R.-J., O'Dowd, C., Ceburnis, D.: Seasonal trends of aerosol hygroscopicity and mixing state in clean marine and polluted continental air masses over the Northeast Atlantic, Journal of Geophysical Research: Atmospheres., 126, e2020JD033851, https://doi.org/10.1029/2020JD033851, 2021.